Magnetic Resonance Imaging 62 (2019) 87–93

Contents lists available at ScienceDirect

Magnetic Resonance Imaging

journal homepage: www.elsevier.com/locate/mri

Original contribution

Improved carotid lumen delineation on non-contrast MR angiography using SNAP (Simultaneous Non-Contrast Angiography and Intraplaque Hemorrhage) imaging

Haining Liu[a,*], Jie Sun[a], Daniel S. Hippe[a], Wei Wu[a,b], Baocheng Chu[a], Niranjan Balu[a], Thomas Hatsukami[c], Chun Yuan[a,d,e]

[a] Department of Radiology, University of Washington, Seattle, WA 98109, United States
[b] Tongji Hospital, Tongji Medical College Affiliated to Huazhong University of Science and Technology, Department of Radiology, 1095 Jiefang Avenue, Wuhan 430000, China
[c] Department of Surgery, University of Washington, Seattle, WA 98109, United States
[d] Department of Bioengineering, University of Washington, Seattle, WA 98109, United States
[e] Department of Bioengineering, Tsinghua University, Beijing 100084, China

ARTICLE INFO

Keywords:
Magnetic resonance imaging
MR angiography
Carotid artery
Image segmentation
Intraplaque hemorrhage

ABSTRACT

Purpose: Simultaneous Non-Contrast Angiography and Intraplaque Hemorrhage (SNAP) was developed for improved imaging of intraplaque hemorrhage (IPH). Its signal polarity also allows for non-contrast time-of-flight MR angiography (TOF). This study sought to compare SNAP and TOF in delineating carotid lumen using contrast-enhanced MRA (CE-MRA) as the reference standard.

Materials and methods: Two hundred and eighty-nine matched slices from 15 arteries among 11 subjects (9 males and 2 females, mean age of 72.1 ± 8.6 years) with luminal stenosis on CE-MRA were studied. Cross-sectional slices centered around the carotid bifurcation were matched between the three MRA techniques (SNAP, TOF, and CE-MRA) and classified as slices with or without plaque (focal wall thickness ≥ 1.5 mm) by additional black-blood vessel wall MRI. Lumen area was measured using a Sobel gradient map for TOF and CE-MRA (magnitude images) and a polarity map for SNAP. Agreement between techniques for measuring lumen area and percent stenosis was evaluated using intraclass correlation coefficient (ICC) and paired *t*-test.

Results: Among the 289 matched slices, SNAP showed a higher agreement with CE-MRA than TOF for measuring lumen area (ICC: 0.93 vs. 0.83; $p = 0.03$). Agreement with CE-MRA was high for both SNAP and TOF in slices without plaque (ICC: 0.91 vs. 0.89; $p > 0.05$) but favored SNAP over TOF in slices with plaque (ICC: 0.93 vs. 0.80; $p = 0.02$).

Conclusion: SNAP, assisted by signal polarity information, demonstrated a higher agreement with CE-MRA in delineating carotid lumen compared to TOF, particularly in slices with plaque where flow conditions may be more complex.

1. Introduction

Luminal stenosis is widely used to guide clinical management in patients with carotid atherosclerosis. Surgical intervention is commonly indicated in symptomatic patients with ≥70% [1] stenosis. However, plaque rupture, which triggers thrombosis and/or thromboembolism, has been recognized as the predominant mechanism for ischemic stroke [2] rather than chronic occlusion. Considerable attention has been directed toward intraplaque hemorrhage (IPH) [3,4], which destabilizes atherosclerotic plaque and may provide incremental prognostic information in stroke risk assessment [5].

Luminal stenosis is measurable with various imaging modalities. However, IPH is currently only detectable with MRI, attributable to the strong T1-shortening effect of methemoglobin generated from

Abbreviations: IPH, intraplaque hemorrhage; CE-MRA, Contrast-enhanced MR angiography; TOF, time-of-flight; SNAP, Simultaneous Non-Contrast Angiography and Intraplaque Hemorrhage; PSIR, phase sensitive inversion recovery; MERGE, prepared Rapid Gradient Echo; ICC, intraclass correlation coefficient; CI, confidence intervals; MIP, maximum intensity projection

* Corresponding author at: 850 Republican St Rm 124, Seattle, WA 98109, United States.
E-mail addresses: pinkney03@gmail.com, hnliu03@gmail.com (H. Liu).

https://doi.org/10.1016/j.mri.2019.06.012
Received 19 March 2019; Received in revised form 20 June 2019; Accepted 22 June 2019

erythrocyte degradation [6,7]. As such, an MRI approach to carotid disease evaluation appears appealing. Contrast-enhanced MR angiography (CE-MRA) is an established technique that provides accurate stenosis measurement in the carotid artery [8,9]. Nonetheless, the reliance on gadolinium chelates may limit its use, particularly in low-risk patients who need regular follow-up imaging to monitor disease progression [10,11].

Among non-contrast alternatives to CE-MRA, time-of-flight (TOF) is the current standard technique [12], with some capability of detecting IPH due to its inherent T1 contrast [13,14]. Limitations include its susceptibility to flow artifacts, low sensitivity to IPH, and inability to differentiate juxtaluminal IPH from ulceration [13,14]. Simultaneous Non-Contrast Angiography and Intraplaque Hemorrhage (SNAP) imaging is a recently developed phase sensitive MRI technique for improved detection of IPH [15,16]. Unlike TOF, which relies on fast flow refreshment to produce lumen contrast, SNAP utilizes a reference scan to restore the true phase (0, π) of inversion-recovery T1-weighted images [15], which is similar to phase sensitive inversion recovery (PSIR) in myocardial imaging [17]. Using optimized acquisition parameters from previous simulation work, the polarities of static tissue and carotid lumen are reconstructed as positive and negative, respectively [15]. This extra polarity contrast may then be used for carotid lumen delineation.

Using CE-MRA as the reference standard, this study sought to perform a head-to-head comparison between SNAP and TOF for delineating the carotid lumen. We hypothesized that signal polarity information may allow SNAP to provide more accurate measurements of carotid lumen than TOF.

2. Material and methods

2.1. Subjects

Subjects in this retrospective study were recruited as part of a prospective study on the natural history of carotid atherosclerosis [18]. Patients with 16–79% asymptomatic stenosis in at least one carotid artery by duplex ultrasound were recruited from outpatient clinics and vascular ultrasound laboratories at the University of Washington Medical Center and Affiliated Hospitals. All patients underwent 3D carotid MRI (see MR imaging for details). For those without contraindications to gadolinium chelates and willing to participate in this study, a traditional first-pass CE-MRA was performed. To enrich our study sample with disturbed flow conditions, the first 15 carotid arteries that showed luminal stenosis (> 0%) on CE-MRA were included [19]. These arteries were from 11 patients (72.1 ± 8.6 years; 9 males). Institutional review board approval and written informed consent were obtained for all subjects prior to enrollment.

2.2. MR imaging

All MR examinations were performed on a 3.0 T whole-body Philips Ingenia scanner (Philips Healthcare, Best, The Netherlands) at the University of Washington Bio-Molecular Imaging Center, Seattle, USA. An eight-channel phase-array surface coil (Chenguang, Shanghai, China) was used for carotid MRI. SNAP was performed in the coronal plane with the following parameters: TR/TE = 10.0/4.8 ms, TI = 500 ms, flip angle = 11°, FOV = 160 mm (head-to-foot) × 160 mm (right-to-left) × 32 mm (anterior-to-posterior), resolution = 0.8 × 0.8 × 0.8 mm^3, NEX = 2, scan time = 5.3 min. Temporal parameters of SNAP were previously optimized to maximize IPH-to-wall and wall-to-lumen contrast [15]. A 3D TOF sequence was performed in the transverse plane with the following parameters: TR/TE = 20.0/4.9 ms, flip angle = 20°, FOV = 160 mm (right-to-left) × 160 mm (anterior-to-posterior) with transversal resolution of 0.6 × 0.6 mm^2, longitudinal coverage = 48 mm, NEX = 1, scan time = 2.1 min. Also included was a large-coverage, black-blood sequence (Motion-Sensitized Driven Equilibrium (MSDE)- prepared Rapid Gradient Echo, or MERGE) [20] for characterizing the distribution of carotid atherosclerosis. MERGE imaging parameters were as follows: TR/TE = 10.0/4.0 ms, flip angle = 6°, field-of-view = 250 mm (head-to-foot) × 250 mm (right-to-left) × 42 mm (anterior-to-posterior), resolution = 0.8 × 0.8 × 0.8 mm^3, NEX = 2, scan time = 5.3 min. CE-MRA was performed using the embedded body coil. Imaging parameters were: TR/TE = 5.5/1.7 ms, flip angle = 30°, FOV = 350 mm (head-to-foot) × 350 mm (right-to-left) × 64 mm (anterior-to-posterior), resolution = 0.8 × 0.8 × 0.8 mm^3. A gadolinium-based contrast agent (Magnevist, Bayer Healthcare, Wayne, NJ; 0.1 mmol/kg) was used, injected at a rate of 2 ml/s followed by saline flush.

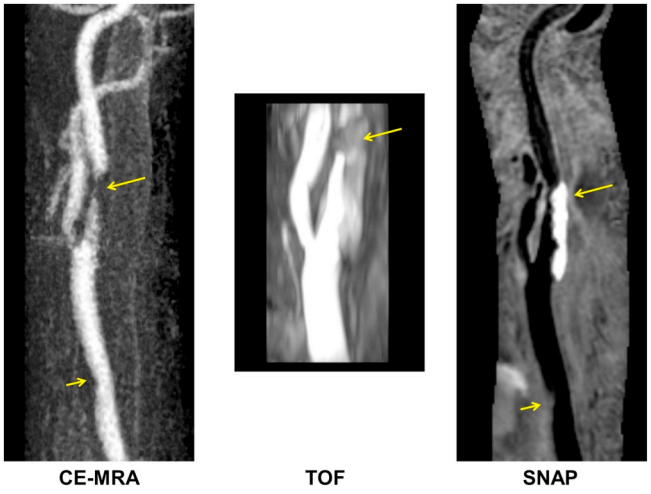

Fig. 1. CE-MRA, TOF, SNAP images of a severe carotid stenosis. For optimal visualization, CE-MRA and TOF are reconstructed with maximum intensity projection and SNAP is reconstructed with curved planar reformation. Long arrows point to the internal carotid artery lesion with intraplaque hemorrhage (hyperintense on SNAP). Short arrows point to another lesion in the common carotid artery, which could be seen on SNAP but not TOF because of the larger coverage of SNAP.

2.3. Image review

Fig. 1 shows 3D reconstructions of CE-MRA, TOF, and SNAP of the same carotid artery. A custom-designed image analysis software package (CASCADE, University of Washington, Seattle, WA) [21] was used for image analysis. To facilitate matching between different sequences, coronally acquired 3D images (SNAP and MERGE) were reformatted into axial slices with a 2 mm slice thickness. The carotid artery bifurcation served as a fiducial marker to match all cross-sectional series. For each sequence, the same 21 slices centered at carotid bifurcation (10 consecutive slices proximal to carotid bifurcation, 1 slice at the bifurcation level, 10 consecutive slices distal to carotid bifurcation) were included in image analysis.

TOF, SNAP and CE-MRA images were read independently in three separate sessions. In each reading session, all available cross-sectional slices were pooled and randomized so that each slice was interpreted independently without the possibility of referencing to anatomically adjacent slices. Reference maps, as an honest reflection of image contrast, were used to obtain objective measures of the carotid lumen. The reference map in TOF and CE-MRA was a gradient map generated with the Sobel operator [22,23], as the differentiation between carotid lumen and wall is primarily based on magnitude information. The lumen boundary was defined along the highest gradient (Fig. 2). The reference map used in SNAP was a polarity map, as the differentiation between carotid lumen and wall is primarily based on polarity information. The lumen boundary was defined around the region with

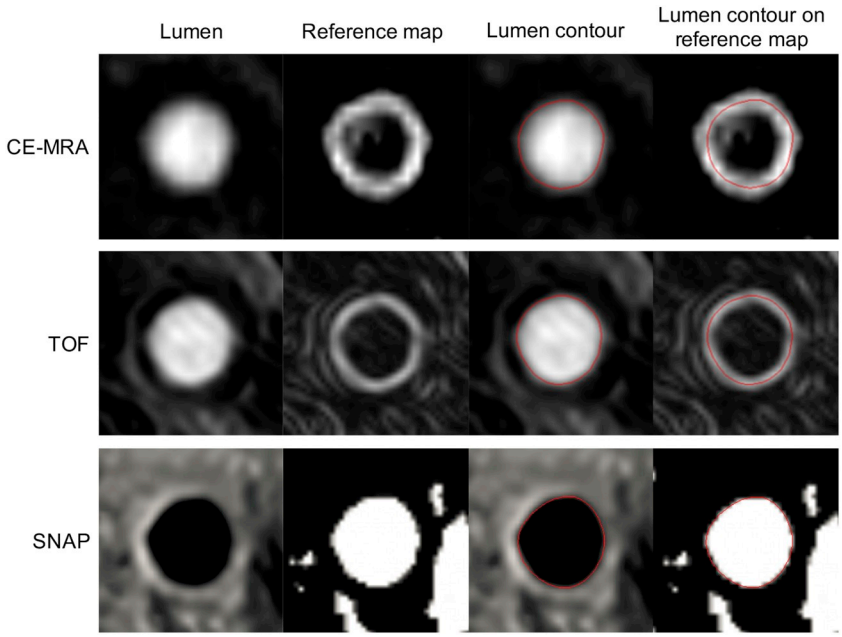

Fig. 2. Comparison between CE-MRA, TOF and SNAP in the delineation of carotid lumen. The first two columns show original images and corresponding reference maps. Reference maps in CE-MRA and TOF are gradient maps generated with the Sobel filter. Reference map in SNAP is a polarity map that marks regions with negative signal. The last two columns show lumen boundaries defined based on reference maps. The lumen boundary is defined along the highest gradient in CE-MRA and TOF and around the region with negative polarity in SNAP.

Table 1
Comparing lumen area measurements between TOF and CE-MRA.

		Sequence[a]					
	Slices (N)	TOF	CE-MRA	Difference[a]	P value[b]	ICC	95% CI
All slices	289	30.3 ± 15.0	32.9 ± 15.8	−2.6 ± 8.7	< 0.001	0.83	0.70, 0.93
With plaque	137	27.6 ± 17.1	32.7 ± 19.0	−5.1 ± 10.6	< 0.001	0.80	0.60, 0.93
Without plaque	152	32.7 ± 12.5	33.1 ± 12.3	−0.4 ± 5.7	0.45	0.89	0.83, 0.93

[a] Values are mean ± standard deviation (mm^2);
[b] Test for no difference between TOF and CE-MRA.

negative polarity (Fig. 2).

Independent of MRA image review, cross-sectional MERGE images were reviewed by an experienced reader to classify MR slices into slices with and without plaque based on whether focal wall thickening (≥1.5 mm) was observed [18].

Lumen area was calculated by the software for all cross-sectional slices. Percent luminal stenosis was calculated for each artery as 100% × (minimum lumen area / reference lumen area). The reference lumen area was calculated from a distal normal slice beyond the carotid bulb if the stenosis was seen in the internal carotid artery, or from a proximal normal slice if the stenosis was in the common carotid artery. The matched slices for both minimum lumen area and referenced lumen area were used for percent luminal stenosis calculations for TOF, SNAP and CE-MRA.

2.4. Statistical analysis

The unit of analysis was an MR slice in analyses of lumen area measurements and an artery in analyses of percent luminal stenosis. Agreement of TOF and SNAP with CE-MRA was assessed using intraclass correlation coefficient (ICC) and a scatter plot. Bias and limits of agreement were evaluated using the Bland-Altman plot (difference versus mean between two sequences). The non-parametric bootstrap and percentile methods were used to calculate 95% confidence intervals (CI) and compare ICC estimates between the two sequences. Resampling was performed per subject to account for dependence between slices from the same subject. Biases in lumen area and percent luminal stenosis relative to CE-MRA were tested against 0 using a permutation test based on the paired *t*-test, where permuting was done per subject. Statistical analysis was performed with Matlab (R2014b, Mathworks, Natrick, MA).

3. Results

Eighteen slices were outside the limited foot-to-head coverage of TOF, and the carotid lumen was partially out of the field-of-view on eight cross-sectional SNAP images due to the limited anterior-to-posterior coverage. A total of 289 matched slices were fully analyzed by all three MRA sequences. Among them, 137 slices (47%) had plaque detected on MERGE images.

3.1. Agreement in lumen area between TOF and CE-MRA

As shown in Table 1 and Fig. 3a, the ICC of the overall agreement between TOF and CE-MRA in measuring lumen area was 0.83 (95% CI: 0.70, 0.93). The agreement appeared to be lower in slices with plaque (ICC: 0.80; 95% CI: 0.60, 0.93) and higher in slices without plaque (ICC: 0.89; 95% CI: 0.83, 0.93). Lumen area measured on TOF was smaller than that measured on CE-MRA, with a negative bias of $-2.6\,mm^2$ ($p < 0.001$; Figs. 4–5). Negative bias was seen primarily in slices with plaque ($-5.1\,mm^2$; $p < 0.001$) and was not apparent in slices without plaque ($-0.4\,mm^2$; $p = 0.45$).

3.2. Agreement in lumen area between SNAP and CE-MRA

The ICC of the overall agreement between SNAP and CE-MRA in measuring lumen area was 0.93 (95% CI: 0.89, 0.96) (Table 2 and Fig. 3b), representing a significant improvement over the agreement

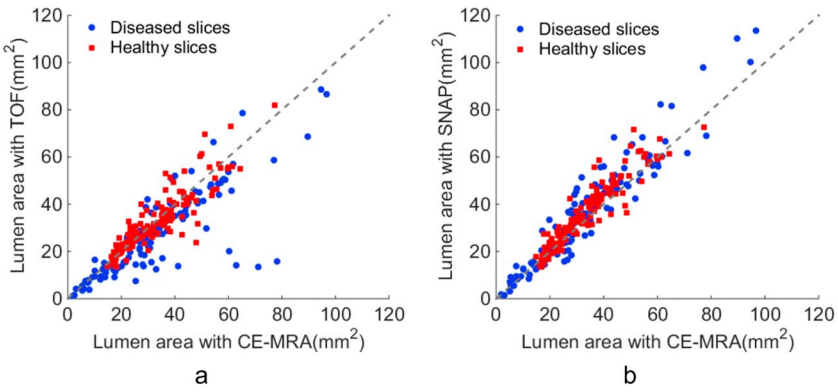

Fig. 3. Scatter plots on agreement of TOF and SNAP with CE-MRA in measuring carotid lumen area. A total of 289 matched MR slices were included, 137 (47%) of which had plaque detected in black-blood vessel wall MRI (blue dots). ICC was 0.83 (95% CI: 0.70, 0.93) for TOF (a) and 0.93 (95% CI: 0.89, 0.96) for SNAP (b). (For interpretation of the references to colour in this figure legend, the reader is referred to the web version of this article.)

between TOF and CE-MRA ($p = 0.03$). Agreement between SNAP and CE-MRA was consistent in slices with (ICC: 0.93; 95% CI: 0.90, 0.96; $p = 0.02$ compared to TOF) and without plaque (ICC: 0.91; 95% CI: 0.86, 0.96; $p > 0.05$ compared to TOF). Lumen area measured on SNAP was larger than that measured on CE-MRA, with a positive bias of $+2.9\,mm^2$ ($p < 0.001$; Fig. 4). The positive bias was similar in slices with ($+3.1\,mm^2$; $p < 0.001$) and without plaque ($+2.8\,mm^2$; $p < 0.001$).

3.3. Percent stenosis measurement

Percent luminal stenosis calculated based on lumen area measurements showed a high agreement with CE-MRA for both TOF (ICC: 0.88; 95% CI: 0.67, 0.96) and SNAP (ICC: 0.94; 95% CI: 0.82, 0.98) (Table 3). The mean differences in percent luminal stenosis compared with CE-MRA were +4.0% ($p = 0.08$) for TOF and +1.5% ($p = 0.46$) for SNAP.

4. Discussion

In this study, the accuracy of carotid lumen delineation by SNAP was compared with TOF, the current choice for non-contrast MRA, using CE-MRA as the reference standard. Major findings are: 1) Lumen area measured on SNAP based on polarity maps showed a higher

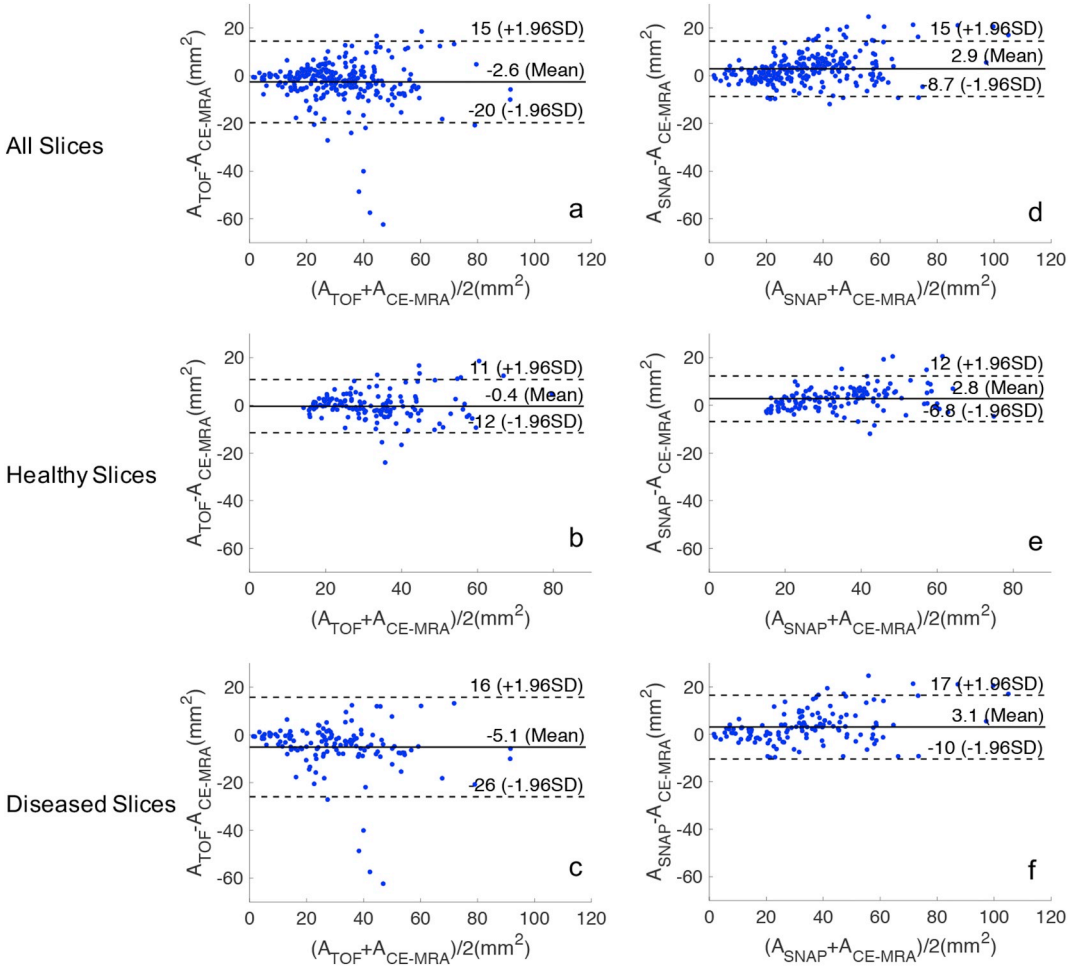

Fig. 4. Bland-Altman plots comparing lumen area measurements between TOF and CE-MRA (a–c) and between SNAP and CE-MRA (d–f). Matched MR slices (a, d) are categorized as those with plaque (c, f) and those without plaque (b, e). Mean differences and 95% limits of agreements are shown.

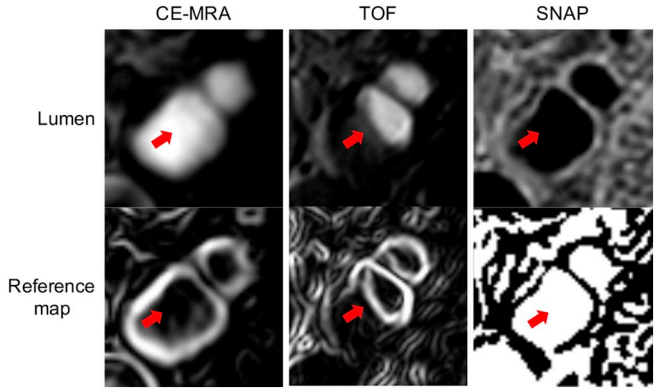

Fig. 5. A representative slice showing flow artifacts in TOF. The top row shows original images of CE-MRA, TOF, and SNAP. The bottom row shows corresponding reference maps. Red arrows indicate a region with turbulent flow that leads to flow artifacts in TOF but not in SNAP. (For interpretation of the references to colour in this figure legend, the reader is referred to the web version of this article.)

agreement with CE-MRA than that measured on TOF based on gradient maps; 2) The agreement and bias of SNAP with CE-MRA were consistent between slices with and without plaque, whereas TOF showed a lower agreement and higher bias relative to CE-MRA in slices with plaque; 3) Compared to lumen areas measured on CE-MRA gradient maps, TOF underestimated lumen area and SNAP overestimated lumen area, both of which appeared to be mitigated by using percent stenosis. This study demonstrates improved carotid lumen delineation by SNAP compared to TOF, indicating the usefulness of polarity information of SNAP in recognizing slow and/or turbulent flow.

The quest for novel non-contrast MRA techniques is primarily driven by two considerations. Despite the low rate of short-term adverse reactions of gadolinium-based contrast media, recent studies demonstrated gadolinium deposition in the central nervous system in a dose-dependent manner, which was relatively independent of renal function [10,11]. While long-term implications of this phenomenon are still under investigation, non-contrast techniques that are able to provide sufficient information for clinical decision-making can be more widely applied in various clinical scenarios. This is particularly relevant for carotid disease, which is a slow progressing disease and often needs regular follow-up imaging. There is also considerable interest in incorporating high-risk plaque features to improve the cost-effectiveness of clinical management of carotid disease [3,5]. It is well recognized that luminal stenosis represents only one aspect of atherosclerotic plaques that is related to clinical risk. IPH imaging has the potential to contribute to a more precise assessment of clinical risk [24]. Existing MRA techniques have some capability of detecting IPH but are prone to false negatives and false positives due to suboptimal IPH contrast and lack of fat suppression. Additionally, quantitative imaging of IPH using these techniques is difficult [14].

TOF is a non-contrast MRA technique widely used in the carotid artery. Image contrast is determined by TR of the radiofrequency acquisition pulse and the refreshment rate of blood within the field-of-view. Due to the short TR of TOF (25–50 ms) [12], slow or turbulent flow may experience more radiofrequency pulses, which deteriorates lumen contrast in focal regions. In our study, TOF underestimated lumen area in slices with plaque. It is conceivable that the presence of underlying atherosclerosis may result in complex flow conditions around the carotid bifurcation, exemplifying the limitations of TOF contrast mechanism. In a previous study, Kramer et al. [25] compared TOF and CE-MRA in measuring cross-sectional lumen area at three levels around the carotid bifurcation (2 cm proximal, origin of internal carotid artery, 2 cm distal). TOF showed comparable lumen area measurements at proximal and distal levels but exhibited a significant bias at the level of the carotid bifurcation, which is similar to our findings.

SNAP, developed based on the widely used PSIR technique [17] in myocardial imaging, can be implemented on major MRI systems. It uses an extra inversion-recovery preparation pulse to generate image contrast [15]. The long interval between inversion pulses (about 2 s) allows more complete blood refreshment within the field-of-view. Therefore, SNAP may be less susceptible to slow or turbulent flow. The added polarity doubles the dynamic range of image contrast and allows lumen boundaries to be defined by the region with negative polarity. In our study, SNAP demonstrated a consistent agreement with CE-MRA in slices with and without plaques. Notably, lumen area measured on SNAP based on polarity maps was larger than that measured on CE-MRA based on gradient maps, and was consistently seen in slices with and without plaques. This difference may be due to a systemic bias between the reference maps in determining lumen boundaries. A possible explanation is that the highest gradient of image contrast on CE-MRA is typically located within the true lumen boundary. In calculating percent luminal stenosis, such systemic biases were canceled out in ratios and did not cause a significant difference between SNAP and CE-MRA. Although not a focus of this investigation, another advantage of SNAP over TOF is the larger longitudinal coverage (16 cm vs. 4.8 cm), which may allow SNAP to capture atherosclerosis beyond the bifurcation segment. The scan time of TOF will have to be tripled to achieve a similar coverage to SNAP. On the other hand, despite the higher scan efficiency of SNAP, shorter total scan times are always desirable. Given the sparsity of polarity maps, SNAP may be well suited for accelerated acquisition using compressed sensing [26], which warrants further investigation.

This study compared MRA contrast mechanisms between TOF and SNAP. Two rigorous measures were taken to minimize influences from human readers so that the obtained measurements objectively reflected the robustness and limitations of each technique in delineating carotid lumen in the presence of complex flow conditions. First, all cross-

Table 3
Measurements of percent luminal stenosis (N = 15).

	Stenosis[a]	Bias relative to CE-MRA[a]	P value[b]	ICC (95% CI)
CE-MRA	52 ± 20%	NA	NA	NA
TOF	56 ± 19%	4.0 ± 9%	0.08	0.88 (0.67, 0.96)
SNAP	54 ± 22%	1.5 ± 7%	0.46	0.94 (0.82, 0.98)

[a] Values are mean ± standard deviation.
[b] Test for no difference between SNAP/TOF and CE-MRA.

Table 2
Comparing lumen area measurements between SNAP and CE-MRA.

		Sequence[a]					
	Slices (N)	SNAP	CE-MRA	Difference[a]	P value[b]	ICC	95% CI
All slices	289	35.8 ± 18.0	32.9 ± 15.8	2.9 ± 5.9	< 0.001	0.93	0.89, 0.96
With plaque	137	35.7 ± 21.8	32.7 ± 19.0	3.1 ± 6.9	< 0.001	0.93	0.90, 0.96
Without plaque	152	35.8 ± 13.9	33.1 ± 12.3	2.8 ± 4.9	< 0.001	0.91	0.86, 0.96

[a] Values are mean ± standard deviation (mm^2);
[b] Test for no difference between SNAP and CE-MRA.

sectional MR slices were pooled and analyzed in random without referencing anatomically adjacent slices. As such, readers' experience in recognizing flow artifacts by referencing to adjacent slices did not take effect, eliminating biases. Second, reference maps were generated based on the contrast mechanisms of MRA techniques, which were used to objectively define lumen boundaries. Such reference maps have the potential to be used in developing semi-automatic algorithms for obtaining area-based stenosis measurements. Currently, maximum intensity projection (MIP) reconstructions are often used for measuring diameter-based stenosis because manual measurements are more convenient to obtain on MIP images [27]. However, fine structures in the stenotic region may be lost [28] and luminal stenosis can be underestimated when the shape of the lumen is asymmetric [29]. The high agreement between SNAP and CE-MRA in measuring lumen areas using reference maps indicates the possibility of developing more automated methods for evaluating luminal stenosis based on lumen area measurements, which may be more relevant from the hemodynamic perspective. Also, the methodology used in this study may be implementable in other phase sensitive reconstruction applications [17,30].

This study has several limitations. First, the number of patients studied was relatively small. Analyses were designed a priori to be performed at the slice level, considering that complex flow conditions may be present locally and cause subtle differences in lumen area measurements. Second, CE-MRA was used as the reference standard. 3D rotational angiography is a better reference standard for measuring luminal stenosis. However, patients in this study were not candidates for intra-arterial angiography. Furthermore, matching between different techniques is more accurate and convenient if CE-MRA is used as the reference. Lumen contrast in CE-MRA depends primarily on T1 differences induced by gadolinium contrast. Therefore, CE-MRA provides a suitable reference for comparing different non-contrast MRA techniques, as supported by previous studies showing a good agreement between intra-arterial angiography and CE-MRA [8,29]. Third, this study did not study other non-contrast MRA techniques beyond TOF. TOF is the current clinical standard of non-contrast MRA. Furthermore, the goal is to find a non-contrast MRA approach that provides accurate information on both luminal stenosis and IPH. Other non-contrast MRA techniques may have advantages over TOF but have not demonstrated capability of detecting IPH. Finally, this study focused on lumen boundary delineation and did not evaluate performance of these techniques in detecting IPH, due to the lack of a reference standard such as histology. Further studies are needed to compare different T1-weighted sequences for IPH detection.

5. Conclusions

With signal polarity information, SNAP demonstrated a higher agreement with CE-MRA than TOF in measuring carotid lumen area, particularly in slices with plaque where flow conditions may be more complex. SNAP MRA has potential as a non-contrast MRA alternative to TOF in the clinical management of carotid disease.

Declaration of Competing Interest

Daniel S. Hippe has received grants from GE Healthcare and Philips Healthcare. Thomas Hatsukami has received grants from Philips Healthcare. Chun Yuan has received grants from Philips Healthcare and is a Member of Radiology Advisory Network of Philips Healthcare. Niranjan Balu has received grants from Philips Healthcare. Other authors declare that they have no competing interests.

Acknowledgement

This study is supported by grants from the National Institutes of Health (R01 HL103609 and R01 NS083503) and the American Heart Association (17MCPRP33671077).

References

[1] Chaturvedi S, Sacco RL. How recent data have impacted the treatment of internal carotid artery stenosis. J Am Coll Cardiol 2015;65(11):1134–43.
[2] Spagnoli LG, Mauriello A, Sangiorgi G, Fratoni S, Bonanno E, Schwartz RS, et al. Extracranial thrombotically active carotid plaque as a risk factor for ischemic stroke. JAMA 2004;292(15):1845–52.
[3] Moody AR, Singh N. Incorporating carotid plaque imaging into routine clinical carotid magnetic resonance angiography. Neuroimaging Clin N Am 2016;26(1):29–44.
[4] Yoshimura S, Yamada K, Kawasaki M, Asano T, Kanematsu M, Takamatsu M, et al. High-intensity signal on time-of-flight magnetic resonance angiography indicates carotid plaques at high risk for cerebral embolism during stenting. Stroke 2011;42(11):3132–7.
[5] Gupta A, Mushlin AI, Kamel H, Navi BB, Pandya A. Cost-effectiveness of carotid plaque MR imaging as a stroke risk stratification tool in asymptomatic carotid artery stenosis. Radiology 2015;277(3):763–72.
[6] Moody AR, Murphy RE, Morgan PS, Martel AL, Delay GS, Allder S, et al. Characterization of complicated carotid plaque with magnetic resonance direct thrombus imaging in patients with cerebral ischemia. Circulation 2003;107(24):3047–52.
[7] Cappendijk VC, Cleutjens KB, Heeneman S, Schurink GW, Welten RJ, Kessels AG, et al. In vivo detection of hemorrhage in human atherosclerotic plaques with magnetic resonance imaging. J Magn Reson Imaging 2004;20(1):105–10.
[8] Wardlaw JM, Chappell FM, Best JJ, Wartolowska K, Berry E, Research NHS, et al. Non-invasive imaging compared with intra-arterial angiography in the diagnosis of symptomatic carotid stenosis: a meta-analysis. Lancet 2006;367(9521):1503–12.
[9] Remonda L, Senn P, Barth A, Arnold M, Lovblad KO, Schroth G. Contrast-enhanced 3D MR angiography of the carotid artery: comparison with conventional digital subtraction angiography. AJNR Am J Neuroradiol 2002;23(2):213–9.
[10] Kanda T, Fukusato T, Matsuda M, Toyoda K, Oba H, Kotoku J, et al. Gadolinium-based contrast agent accumulates in the brain even in subjects without severe renal dysfunction: evaluation of autopsy brain specimens with inductively coupled plasma mass spectroscopy. Radiology 2015;276(1):228–32.
[11] McDonald RJ, McDonald JS, Kallmes DF, Jentoft ME, Murray DL, Thielen KR, et al. Intracranial gadolinium deposition after contrast-enhanced MR imaging. Radiology 2015;275(3):772–82.
[12] Miyazaki M, Lee VS. Nonenhanced MR angiography. Radiology 2008;248(1):20–43.
[13] Qiao Y, Etesami M, Malhotra S, Astor BC, Virmani R, Kolodgie FD, et al. Identification of intraplaque hemorrhage on MR angiography images: a comparison of contrast-enhanced mask and time-of-flight techniques. AJNR Am J Neuroradiol 2011;32(3):454–9.
[14] Yamada K, Song Y, Hippe DS, Sun J, Dong L, Xu D, et al. Quantitative evaluation of high intensity signal on MIP images of carotid atherosclerotic plaques from routine TOF-MRA reveals elevated volumes of intraplaque hemorrhage and lipid rich necrotic core. J Cardiovasc Magn Reson 2012;14:81.
[15] Wang J, Bornert P, Zhao H, Hippe DS, Zhao X, Balu N, et al. Simultaneous non-contrast angiography and intraplaque hemorrhage (SNAP) imaging for carotid atherosclerotic disease evaluation. Magn Reson Med 2013;69(2):337–45.
[16] Shu H, Sun J, Hatsukami TS, Balu N, Hippe DS, Liu H, et al. Simultaneous non-contrast angiography and intraplaque hemorrhage (SNAP) imaging: comparison with contrast-enhanced MR angiography for measuring carotid stenosis. J Magn Reson Imaging 2017;46(4):1045–52.
[17] Kellman P, Arai AE, McVeigh ER, Aletras AH. Phase-sensitive inversion recovery for detecting myocardial infarction using gadolinium-delayed hyperenhancement. Magn Reson Med 2002;47(2):372–83.
[18] Sun J, Canton G, Balu N, Hippe DS, Xu D, Liu J, et al. Blood pressure is a major modifiable risk factor implicated in pathogenesis of intraplaque hemorrhage: an in vivo magnetic resonance imaging study. Arterioscler Thromb Vasc Biol 2016;36(4):743–9.
[19] Rothwell PM, Eliasziw M, Gutnikov SA, Fox AJ, Taylor DW, Mayberg MR, et al. Analysis of pooled data from the randomised controlled trials of endarterectomy for symptomatic carotid stenosis. Lancet 2003;361(9352):107–16.
[20] Balu N, Yarnykh VL, Chu B, Wang J, Hatsukami T, Yuan C. Carotid plaque assessment using fast 3D isotropic resolution black-blood MRI. Magn Reson Med 2011;65(3):627–37.
[21] Kerwin W, Xu D, Liu F, Saam T, Underhill H, Takaya N, et al. Magnetic resonance imaging of carotid atherosclerosis: plaque analysis. Top Magn Reson Imaging 2007;18(5):371–8.
[22] Qiao Y, Steinman DA, Etesami M, Martinez-Marquese A, Lakatta EG, Wasserman BA. Impact of T2 decay on carotid artery wall thickness measurements. J Magn Reson Imaging 2013;37(6):1493–8.
[23] Greenman RL, Wang X, Ngo L, Marquis RP, Farrar N. An assessment of the sharpness of carotid artery tissue boundaries with acquisition voxel size and field strength. Magn Reson Imaging 2008;26(2):246–53.
[24] Hosseini AA, Kandiyil N, Macsweeney ST, Altaf N, Auer DP. Carotid plaque hemorrhage on magnetic resonance imaging strongly predicts recurrent ischemia and stroke. Ann Neurol 2013;73(6):774–84.
[25] Kramer H, Runge VM, Morelli JN, Williams KD, Naul LG, Nikolaou K, et al. Magnetic resonance angiography of the carotid arteries: comparison of unenhanced and contrast enhanced techniques. Eur Radiol 2011;21(8):1667–76.
[26] Lustig M, Donoho D, Pauly JM. Sparse MRI: the application of compressed sensing for rapid MR imaging. Magn Reson Med 2007;58(6):1182–95.

[27] Runck F, Steiner RP, Bautz WA, Lell MM. MR imaging: influence of imaging technique and postprocessing on measurement of internal carotid artery stenosis. AJNR Am J Neuroradiol 2008;29(9):1736–42.
[28] Anderson CM, Saloner D, Tsuruda JS, Shapeero LG, Lee RE. Artifacts in maximum-intensity-projection display of MR angiograms. AJR Am J Roentgenol 1990;154(3):623–9.
[29] Anzalone N, Scomazzoni F, Castellano R, Strada L, Righi C, Politi LS, et al. Carotid artery stenosis: intraindividual correlations of 3D time-of-flight MR angiography, contrast-enhanced MR angiography, conventional DSA, and rotational angiography for detection and grading. Radiology 2005;236(1):204–13.
[30] Liu H, Wilson GJ, Balu N, Maki JH, Hippe DS, Wu W, et al. 3D true-phase polarity recovery with independent phase estimation using three-tier stacks based region growing (3D-TRIPS). MAGMA 2018;31(1):87–99.